TWO-DIMENSIONAL FOURIER TRANSFORM ANALYSIS OF HELICOPTER FLYOVER NOISE

Odilyn L. Santa Maria, F. Farassat
NASA Langley Research Center
Hampton, VA

Philip J. Morris
The Pennsylvania State University
State College, PA

ABSTRACT

A method to separate main rotor and tail rotor noise from a helicopter in flight is explored. Being the sum of two periodic signals of disproportionate, or incommensurate frequencies, helicopter noise is neither periodic nor stationary. The single Fourier transform divides signal energy into frequency bins of equal size. Incommensurate frequencies are therefore not adequately represented by any one chosen data block size. A two-dimensional Fourier analysis method is used to separate main rotor and tail rotor noise. The two-dimensional spectral analysis method is first applied to simulated signals. This initial analysis gives an idea of the characteristics of the two-dimensional autocorrelations and spectra. Data from a helicopter flight test is analyzed in two dimensions. The test aircraft are a Boeing MD902 Explorer (no tail rotor) and a Sikorsky S-76 (4-bladed tail rotor). The results show that the main rotor and tail rotor signals can indeed be separated in the two-dimensional Fourier transform spectrum. The separation occurs along the diagonals associated with the frequencies of interest. These diagonals are individual spectra containing only information related to one particular frequency.

LIST OF SYMBOLS

A Amplitude component of autocorrelation, $R_X(t)$

B Amplitude component of autocorrelation, $R_X(t)$

$E[\bullet]$ Expected value

$\hat{E}$ Fourier transform of expected value

g Variable of characteristic equation

R_x Autocorrelation of signal X

S_x Fourier transform of signal X

t Time

T Period

$X(t)$ Signal, time history

α Frequency variable

β Frequency variable

δ Dirac delta function

λ Frequency variable in 2-D Fourier transform

ω Frequency in radians

Subscripts:

m Integer variable

n Integer variable

I. INTRODUCTION

The sound of a helicopter flying overhead is one that most people can identify. Its distinctive noise is a cause of annoyance to the listener on the ground, and therefore could be considered a high impact community noise source. The first step in the process of reducing far field helicopter noise is its characterization. This involves identifying:

- where on the aircraft the noise is being generated;
- what condition the aircraft is flying when the noise is generated;

Presented at the American Helicopter Society 55th Annual Forum, Montreal, Quebec, May 25 – 27, 1999.

- how the noise propagates to the ground.

This information can be used to create an illustration or graphic that visualizes the acoustics of a helicopter. The graphic could then be a tool used to identify the areas (flight operations, blade tips, etc) to modify in order to reduce the noise for the listener. The researcher is thus challenged to create this illustration or graphic that efficiently conveys the most relevant information.

The purpose of this paper is to identify the advantages of using a 2-D Fourier transform to visualize helicopter flyover noise. Results from this particular 2-D analysis were first introduced in [1].

To explore the possibilities of the 2-D Fourier transform, this paper will provide the 2-D spectra from two different helicopters: one with a tail rotor, and one without. These data, collected during an acoustic flight test in 1996, will be shown using conventional analysis methods, namely the FFT, as well as with the 2-D Fourier transform. The 2-D Fourier transform will be used as an alternate method to distinguish main rotor and tail rotor noise.

Sources of helicopter noise

Figure 1 illustrates the sources of helicopter noise for a helicopter with a tail rotor. These sources of helicopter noise and their physical meaning are defined in [2]. This paper addresses the frequencies associated with main rotor and tail rotor rotation in the helicopter noise spectrum.

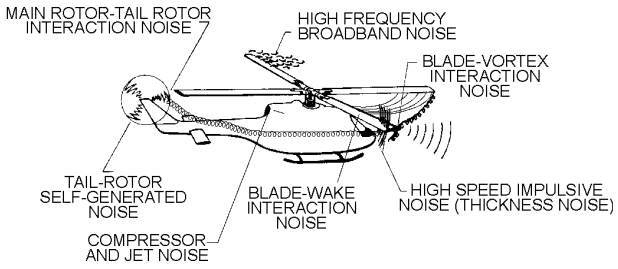

Figure 1. Helicopter noise sources

Noise of the Main Rotor

As shown in Fig. 1, the main rotor generates noise in several ways: 1) high frequency broadband noise, 2) thickness noise, 3) blade-vortex interaction noise, 4) blade-wake interaction noise, 5) loading noise.

Many studies have been conducted to identify, predict, and measure these different sources of main rotor noise. Some studies have targeted the wakes and tip vortices shed by the main rotor blades. These wakes and tip vortices not only generate blade-wake interaction and the highly impulsive blade-vortex interaction noise when they encounter other main rotor blades, but they can also encounter the tail rotor blades and generate main rotor-tail rotor interaction noise.

Noise of the Tail Rotor

The tail rotor itself generates the same types of noise as the main rotor. However, due to its orientation on the aircraft, its surrounding flow field in flight is quite different from that of the main rotor. It is not only ingesting atmospheric turbulence, it is also encountering wakes and vortices from the main rotor, hub, and fuselage. Also, due to its orientation, any noise radiating in the tail rotor tip path plane would propagate to the ground underneath the tail. References [5], [6], [7], and [8] address tail rotor noise. This type of noise was observed to be strongest during takeoff for the Sikorsky S-76 in Ref. [8].

Periodicity of Helicopter Noise

The main rotor-tail rotor ratio, the multiple of tail rotor rotational frequency in relation to the main rotor rotational frequency, is never designed to be a whole number. This prevents the harmonics of the two rotors from reinforcing each other and resonating. Thus the noise from these two rotors can be characterized as the sum of two periodic signals with incommensurate frequencies. It is shown theoretically in [4] that this summed signal is not periodic. Errors described in ref. [9] would result if the 1-D Fourier transform is used on a non-periodic signal. Therefore, Hardin and Miamee proposed in [4] that a 2-D Fourier transform would better characterize the signal.

The following section discusses the 2-D Fourier transform and explains how it may be used to distinguish main rotor noise from tail rotor noise more clearly. Section III shows preliminary 2-D Fourier transform analyses performed on simulated signals to indicate what "ideal" 2-D spectra should look like. Section IV describes the helicopter acoustics flight test from which data is analyzed. Section V shows the results of 2-D Fourier transform analysis on the measured flyover data, followed by conclusions in Section VI. The advantages of 2-D Fourier transform analysis on helicopter flyover acoustic data are also discussed in Section VI.

II. 2-D FOURIER TRANSFORM

The 2-D Fourier transform is defined in ref. [10] as

$$S_x(\lambda_1,\lambda_2)=\int_{-\infty}^{\infty}\int_{-\infty}^{\infty}R_x(t_1,t_2)e^{-j(\lambda_1 t_1+\lambda_2 t_2)}dt_1 dt_2 \qquad (1)$$

$R_x(t_1,t_2)$ is the 2-D autocorrelation of a signal X(t),

$$R_x(t_1,t_2)=E[X(t_1)X(t_2)] \qquad (2)$$

$E[\cdot]$ is the expected value.

In ref. [4], Hardin and Miamee first introduced the 2-D Fourier transform as a possible method to separate main rotor and tail rotor noise. Miamee and Smith [11] developed an estimation of the 2-D spectrum based on the 1-D spectrum. Although this previous work resulted in an increased understanding of the characteristics of the 2-D Fourier transform, separation of incommensurate frequencies was not achieved.

The estimation of the 2-D spectrum used in this paper is based on the 2-D autocorrelation shown in Eq. 2. $R_x(t_1,t_2)$ is calculated using a single sample from a given signal. The 2-D Fourier transform is then calculated using the FFT2 function in the Signal Processing Toolbox of MATLAB. Estimation of the 2-D spectrum from the 2-D autocorrelation resulted in higher tonal resolution than the estimation in [11] which used the 1-D spectrum.

Ref. [1] provides the derivation of the 2-D Fourier transform for a signal of the form

$$X(t)=\sum_n\left(A_n e^{in\omega_1 t}+B_n e^{in\omega_2 t}\right) \qquad (4)$$

where n is the harmonic number, A and B are amplitudes, and ω_1 and ω_2 are incommensurate frequencies. The signal $X(t)$ is the sum of periodic signals with two incommensurate frequencies.

The 2-D Fourier transform of $X(t)$ in Eq. 4 is

$$\hat{E}(\lambda_1,\lambda_2)=\sum_{m=1}^{N}\sum_{n=1}^{N}\begin{bmatrix}A_m A_n\delta(\lambda_1-n\omega_1)\delta(\lambda_2-m\omega_1)\\+A_n B_m\delta(\lambda_1-n\omega_1)\delta(\lambda_2-m\omega_2)\\+A_m B_n\delta(\lambda_1-n\omega_2)\delta(\lambda_2-m\omega_1)\\+B_m B_n\delta(\lambda_1-n\omega_2)\delta(\lambda_2-m\omega_2)\end{bmatrix} \qquad (5)$$

where δ is the Dirac delta function.

Figure 2 shows a schematic of the Dirac delta functions in the 2-D spectrum, which form a series of diagonal lines parallel to the main or center diagonal. The amplitudes of the diagonals illustrated in Fig. 2 are products of different combinations of A_m, A_n, B_m, and B_n. These amplitudes along the main or center diagonal would be for the case $m=n$. It is then possible from these center diagonal amplitudes to break down the different components of the amplitude of the parallel diagonals. This field of amplitude components will not be applied to the data in this paper. It is simply introduced as a subject for further study.

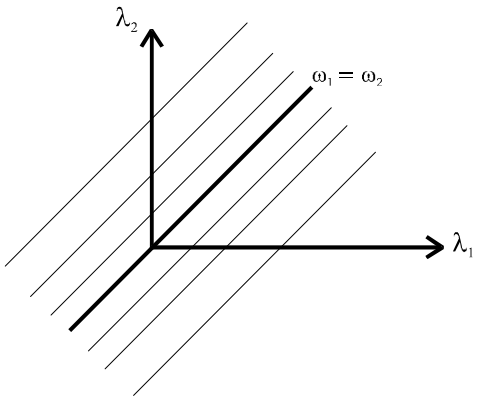

Figure 2. Support of 2-D power spectral density [4].

The next section gives some examples of 2-D Fourier transform spectra from simulated signals. These provide some idea of the characteristics of 2-D spectra of very simple signals, thus giving a simple preview of the expected spectra of real helicopter signals.

III. RESULTS WITH SIMULATED SIGNALS

To get an idea of the expected results from the experimental data, it is useful to work initially with simulated or computer-generated data. In the following subsections, 2-D spectra are shown for a pure tone, a periodically correlated signal, and a non-periodic signal. Since 2-D spectral values are generally complex, the amplitude of the spectra is shown.

All calculations are made using a sampling rate of 5000 Hz and a rectangular window. To enhance the tone levels, the sample lengths are multiples of the fundamental frequency of 20 Hz. Multiples of the fundamental frequency at 20 Hz are used for better resolution.

Pure tone

A simple periodic signal is a sinusoid. Figure 3 shows the time history and 1-D spectrum of a sinusoidal signal

with frequency 20 Hz. The 1-D spectrum in Fig. 3(b) shows a peak at 20 Hz, as expected.

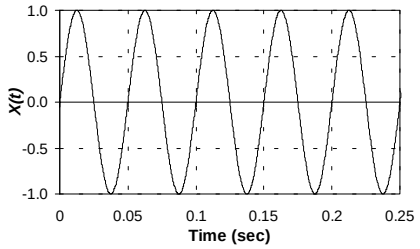

(a) Sinusoidal signal, *X(t)*

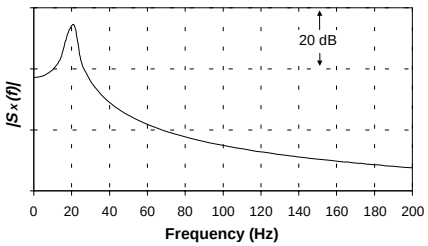

(b) Spectum, $S_x(f)$ of *X(t)*.

Figure 3. Pure tone at 20 Hz, 1-D.

The 2-D autocorrelation and 2-D spectrum of the signal shown in Fig. 3(a) are shown in Fig. 4. The diagonal of the spectrum in Fig. 4 is equivalent to the single Fourier transform spectrum that is shown in Fig. 3(c).

Periodically Correlated Signal

A periodically correlated signal consisting of a pure tone and harmonics with decreasing amplitude has also been generated, using MATLAB. For this example, 19 harmonics in addition to the fundamental at 20 Hz are generated, using the following equation:

$$X(t) = \sum_{i=1}^{20} (1 - .01i) \sin(2\pi 20it) \qquad (6)$$

where t = 0 to 409.4 msec in increments of 0.2 msec.

Figure 5(a) shows that the time history of the signal up to 0.25 sec has a period of 0.05 sec. Figure 5(b) shows the 1-D spectrum of the signal, in which all 20 tones (fundamental plus 19 harmonics) can be observed. This particular example resembles the signal from a helicopter without a tail rotor, such as the MD 902 Explorer.

Figure 6 shows the 2-D autocorrelation and 2-D spectrum of the periodically correlated signal. Figure

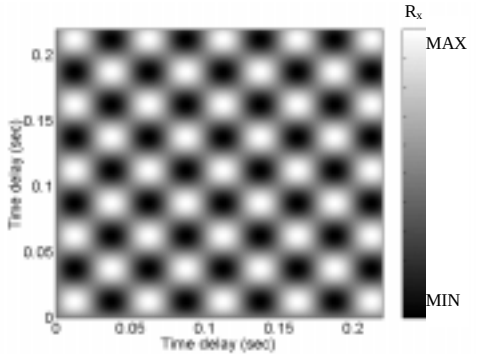

(a) 2-D autocorrelation

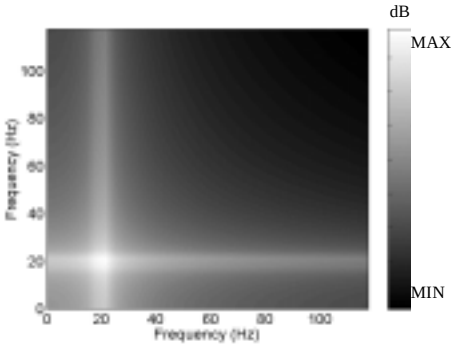

(b) 2-D spectrum

Figure 4. Pure tone at 20 Hz.

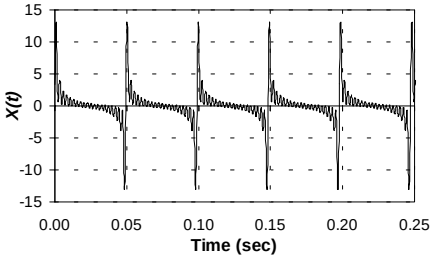

(a) Time history

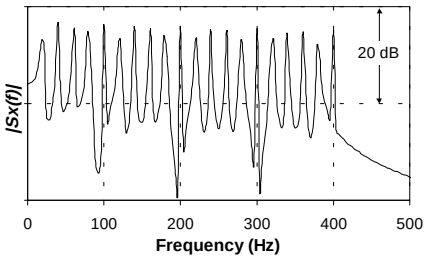

(b) 1-D Spectrum

Figure 5. Periodically correlated signal, 1-D

6(a) shows a matrix of dots, which are equally spaced by the period. The "support" lines described in [4] may

be drawn in Fig. 6(b) connecting the intersections of the white lines parallel to the diagonal.

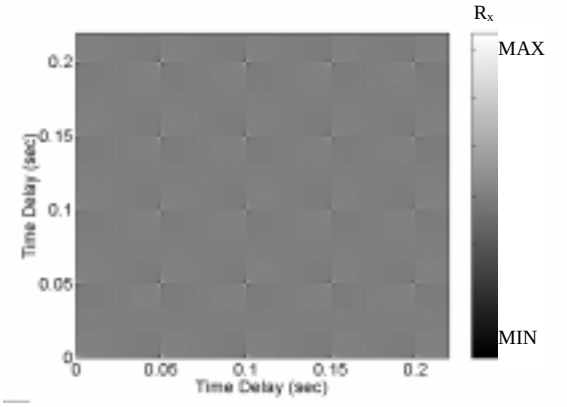

(a) 2-D autocorrelation, Rx(t)

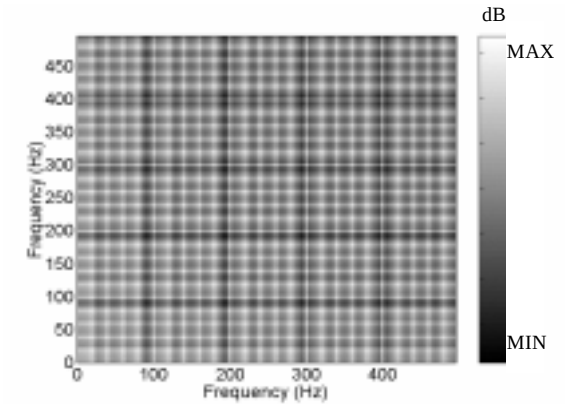

(b) 2-D spectrum

Figure 6. Periodically correlated signal, 2-D.

Incommensurate Frequencies

To simulate a helicopter with a tail rotor, two sinusoidal signals with incommensurate frequencies are summed using the following equation:

$$X(t) = \sum_{i=1}^{30} (1 - 0.01i)\sin(2\pi 20it) + \sum_{j=1}^{5} (1 - 0.01j)\sin\left(2\pi 20\sqrt{30}jt\right) \quad (7)$$

where t = 0 to 409.4 msec in increments of 0.2 msec.

The two frequencies differ by a factor of $\sqrt{30}$ (20 and $20\sqrt{30}$ Hz), which approximates the main rotor-tail rotor ratio of the Sikorsky S-76C helicopter. The 20-Hz harmonics will be referred to as the main rotor tones and the $20\sqrt{30}$ (~110) Hz harmonics will be called the tail rotor tones. The simulated signal includes harmonics with decreasing amplitude for both sinusoids. The time history of this signal is shown in Fig. 7(a). Though it appears periodic in nature, it is in fact non-periodic, as explained in the previous section. Figure 7(b) shows the 1-D spectrum of this non-periodic signal. Note the higher amplitude at 220 Hz, where the 11th and 2nd harmonics, respectively, of the two signals are nearly integer multiples of each other. Because their frequencies are so close, the energy content from both harmonics end up in the same frequency bins at 110-Hz multiples.

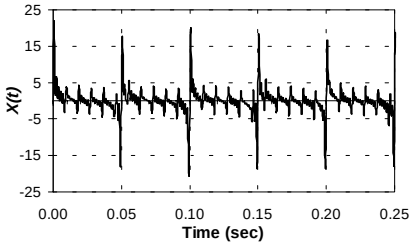

(a) Time history

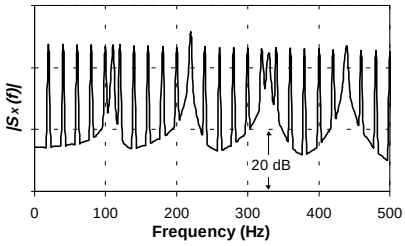

(b) 1-D Spectrum

Figure 7. Periodic signals with incommensurate frequencies, 1-D.

Figure 8 shows the 2-D autocorrelation and spectrum of the simulated non-periodic signal. Close observation of Fig. 8(a) reveals the peaks of the lower (main rotor frequency) represented as dots, and faint "notches" mark the higher (tail rotor) frequency. Fig. 8(b) shows all the frequencies generated in white, including the higher (tail rotor) frequency at multiples of 20 and 110 Hz.

Three diagonals for the center, main rotor, and tail rotor are marked on the 2-D spectrum in Fig. 8(b). The center diagonal is equivalent to the 1-D spectrum and contains information from all the frequencies in the signal. The main rotor diagonal, closest to the center diagonal, would only contain information from the main rotor frequency at 20 Hz. The tail rotor diagonal is parallel to the center diagonal, offset by 110 Hz, and should contain information only from the tail rotor.

Figure 9shows the center diagonal plotted against the main rotor and tail rotor diagonals. In Fig. 9(a), most of the main rotor tones in the main rotor diagonal remain at the same level as in the center diagonal. The first and third harmonics of the tail rotor at 110 and 330 Hz, respectively, are reduced by over 20 dB in the main rotor diagonal. The second harmonic of the tail rotor at 220 Hz is only reduced by 5 dB, and the fourth harmonic at 440 Hz is reduced by 1 dB. As mentioned above, the second and fourth harmonics of the tail rotor nearly coincide with the 11th and 22nd harmonics of the main rotor. Therefore, it appears that in the main rotor diagonal, the energy in those two frequency bins has been reduced by the contribution of the tail rotor.

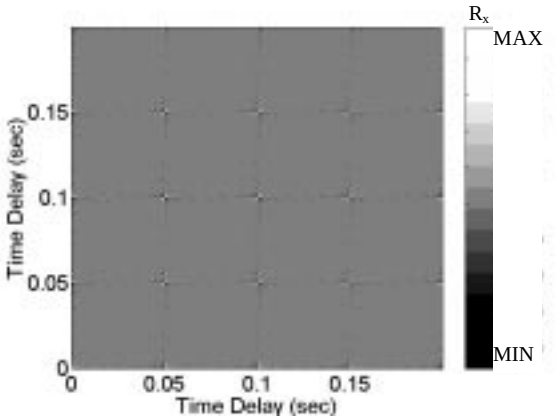

(a) 2-D autocorrelation

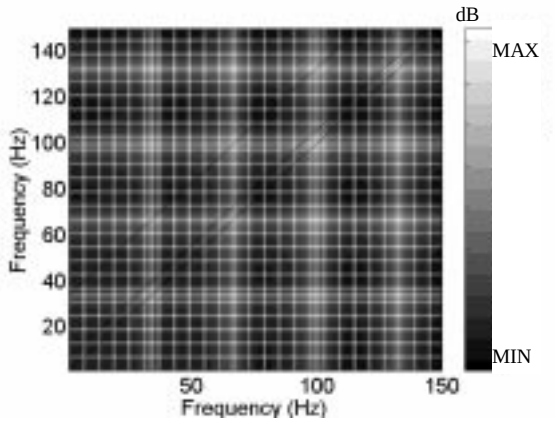

(b) 2-D spectrum

Figure 8. Sum of periodic signals with incommensurate frequencies.

In Fig. 9(b), most of the main rotor tones are reduced by over 30 dB in the tail rotor diagonal. The first and third harmonics of the tail rotor retain their center diagonal levels, while the second harmonic is reduced by 7 dB, the fourth harmonic by 4 dB. The fourth harmonic of the tail rotor is also shifted one frequency bin lower to 437 Hz in the tail rotor diagonal. There are spikes in the tail rotor diagonal halfway between the main rotor tones that are not present in the center diagonal. These minor, or low-level tones represent the diagonal cutting through the white lines seen in Fig. 8(b). The major, or high-level tones appear when the diagonal cuts through an intersection of these white lines. The significance or physical interpretation of these minor tones is not explored in this paper.

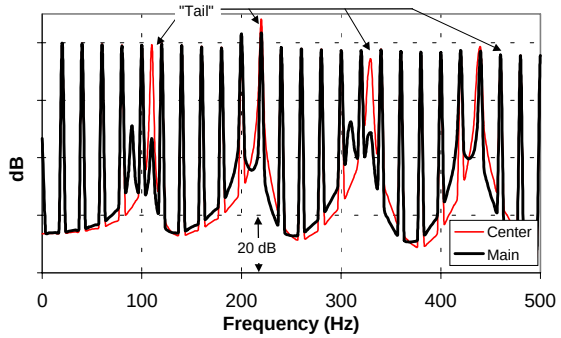

(a) Main rotor diagonal (20 Hz)

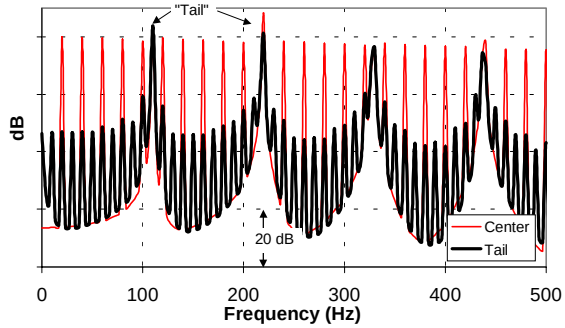

(b) Tail rotor diagonal (~110 Hz)

Figure 9. Diagonals from 2-D spectrum, sum of incommensurate frequencies.

IV. FLIGHT TEST DESCRIPTION

The experimental data used in this paper were acquired during the 1996 Noise Abatement Flight Test sponsored by the National Rotorcraft Technology Center (NRTC) and the Rotorcraft Industry Technology Association (RITA). Participating organizations were NASA Langley and Ames Research Centers, Volpe National Transportation Systems Center (Department of Transportation), Boeing Mesa, and Sikorsky Aircraft. The test was conducted at the NASA Ames Crows Landing Flight Test Facility in Crows Landing, California.

The purpose of the test was to validate the Differential Global Positioning System (DGPS) for precision guidance for acoustic flight testing, with the specific application of designing high precision quieter approaches. For the purpose of this paper, the flight test parameters provided an extensive database of helicopter flyover noise for main rotor-tail rotor interaction analysis. Reference [12] describes the purpose and methodology of the flight test in depth.

Test Aircraft

Among the aircraft tested were a Boeing MD902 Explorer, and a Sikorsky S-76. The Boeing MD902 Explorer, shown in Fig. 10, is a five-bladed, eight-passenger helicopter featuring the NOTAR® anti-torque system (no tail rotor). Its rotor diameter is 33.83 ft, and its maximum takeoff gross weight (MTOGW) is 6250 lbs. Reference [13] describes the Boeing Explorer portion of the flight test.

Figure 10. Boeing MD902 Explorer.

Figure 11 shows the Sikorsky S-76 test aircraft. It is a 4-bladed (44-ft diameter), 10-passenger aircraft with a four-bladed tail rotor (8-ft diameter). Its gross takeoff weight during testing was nominally 11,200 lb, 500 lb less than its MTOGW of 11,700 lb. Reference [14] provides a description and results from the Sikorsky S-76 portion of the flight test.

Figure 11. Sikorsky S-76.

Microphone Layout

The test aircraft flew over a 50-microphone array laid out on agricultural land adjacent to the Crows Landing main runway. Figure 12 is a schematic of the array, which encompassed approximately 1.1 sq. mi. Data was acquired by four different groups: Sikorsky, Boeing Mesa, and Volpe using Sony digital DAT recorders, and NASA Langley using the field digital acquisition system. Microphones labeled N26, N27, and N28 in Fig. 12 are used in this paper. These were selected for their locations along the flight track, and ease of accessing the data. The data from these three microphones were recorded on the same tape by one of the NASA digital systems. They will be referred to as the port (N26), centerline (N27), and starboard (N28) microphones hereafter in this paper.

Due to the proprietary nature of the acoustic data, no absolute dB levels are shown in this paper. To allow comparison of relative levels, scales remain constant between microphones in each set of data.

Flight Parameters

Approaches were flown to a hover over the hover pad, with glideslopes such that the aircraft was at 394 ft altitude when over the reference microphone. Level flyovers were flown at various altitudes. For the S-76, departures began at a nominal 200 ft altitude and 394 ft directly overhead of the reference microphone. No departure or takeoff data were recorded for the MD 902 Explorer.

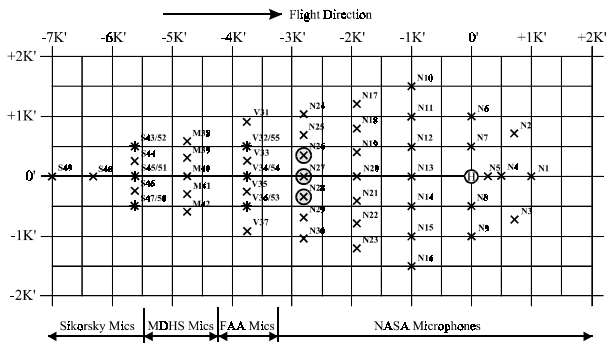

Figure 12. Microphone array layout at Crows Landing, CA, during flight test.

Data Acquisition and Analysis

Data for the three microphones presented in this paper were acquired at a 20 kHz sampling rate. Each data run varied in length, depending on the flight parameters such as glideslope, and speed. For the purposes of this paper, the data used from each flyover were chosen after inspecting their spectrograms. Spectrograms were produced by taking an 8192-point Fast Fourier Transform (FFT) every 4096 points of the signal for a

50% overlap. Figure 14 is an example of a spectrogram of a flyover.

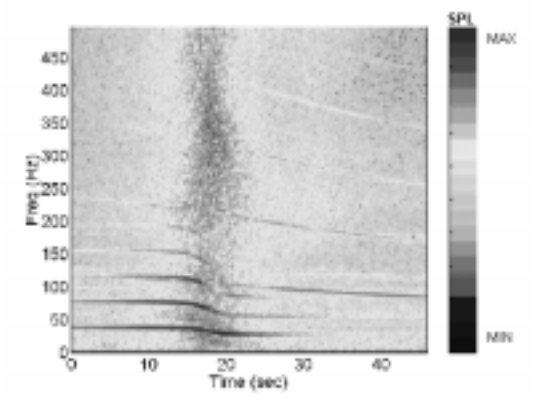

Figure 13. Spectrogram of Boeing MD902 Explorer level flyover recorded by centerline microphone.

The horizontal axis in Fig. 13 denotes time, the vertical axis denotes frequency, and the sound pressure level (SPL) on a decibel scale is denoted by shade. The main rotor tones are seen in Fig. 13 as the dark horizontal lines beginning at about 40 Hz, and spaced about 40 Hz apart. The Doppler shift is seen as the shift in frequency of these main rotor tone lines. The frequency shift is especially severe near the overhead point at approximately 19 seconds into the flyover. Beyond the overhead point, some tones at approximately 200 Hz appear as faint gray and white lines at intervals of about 180 Hz. These tones are apparently radiated aft of the helicopter, since they are not very strong prior to the overhead point. Data segments with high tone levels and low Doppler shift have been selected as the best to represent the noise of the flyover.

V. RESULTS WITH EXPERIMENTAL DATA

The time histories of selected runs from the 1996 Crows Landing flight test have been analyzed using MATLAB software. The first step is to identify, as described in the previous section, a suitable "slice" of data from each selected run. A starting point is then identified in the signal. From this starting point, a segment with a length of an integer multiple of the main rotor period is analyzed.

Table 1 lists the aircraft distances relative to the three microphones used for the start and end of the data segments used in the Fourier analyses. The last column of Table 1 shows the distance traveled by the aircraft during the data set analyzed.

TABLE I
Aircraft Distances from Microphones

	Start Distance (ft) from / End Distance (ft) from			Travel
	Port	Center	Starboard	Dist. (ft)
MD 902 Level	3252 / 3205	3235 / 3187	3255 / 3207	48
S-76 Level	3257 / 3182	3238 / 3161	3256 / 3180	77
S-76 Takeoff	1592 / 1562	1546 / 1515	1579 / 1548	45
S-76 Approach	3285 / 3244	3267 / 3226	3287 / 3247	41

One Dimensional Spectra

Boeing MD 902 Explorer

Figure 14 shows the 1-D spectra of a portion of a Boeing MD 902 Explorer level flyover for the three microphones specified above. As listed in Table 1, the aircraft was approximately 3200 ft away.

The spectra of Fig. 14 show that the noise measured by these microphones was dominated by the main rotor harmonics. The fundamental BPF tones at 39 Hz for all three microphones was about 30 dB above the noise floor. Four harmonics were at least 10 dB above the noise floor from the port and centerline microphones, and 5 harmonics from the starboard microphone. Disregarding the other discernible tones with comparatively low sound pressure level (SPL), the signals whose spectra were shown in Fig. 14 would be considered periodic. Therefore, the 1-D spectrum should be sufficient to describe the noise spectral characteristics of this aircraft.

Sikorsky S-76 – Level Flight

Figure 15 shows the spectra from a Sikorsky S-76 level flight for the three microphones. As with the Boeing MD 902 Explorer, the Sikorsky S-76 was approximately 3200 ft away from the microphones during the data segment shown.

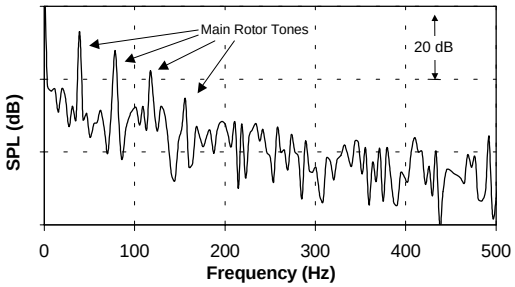

(a) Port Microphone (Retreating Side)

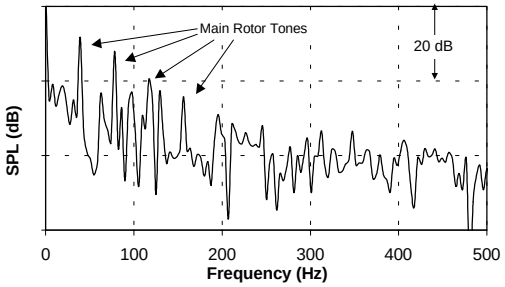

(b) Centerline Microphone

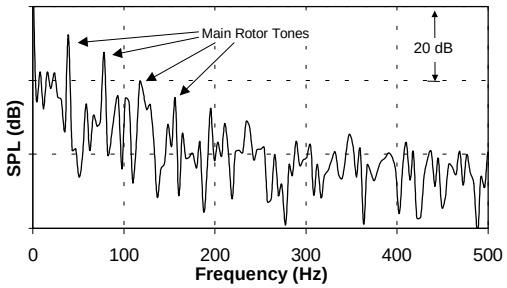

(c) Starboard Microphone (Advancing Side)

Figure 14. Boeing MD902 Explorer spectra for level flight at 115 knots, 500 ft altitude, 3200 ft uprange of mics.

The main rotor tones, beginning at 25 Hz, are dominant in the signals from the 3 microphones. The tail rotor fundamental BPF was 141 Hz. Although 10 – 20 dB lower than the highest levels in the three spectra, the tail rotor tones are discernible and are labeled in Fig. 15. Note that the tail rotor tone at approximately 280 Hz was also a multiple of the main rotor BPF, therefore there was some energy from the main rotor noise in this particular tone.

Sikorsky S-76 – Takeoff

Figure 16 shows the 1-D spectra from the three microphones for a Sikorsky S-76 takeoff. Table 1 lists the distance from the microphones as approximately 1500 ft. As mentioned in Section III, reference [8] indicated a stronger tail rotor signal during takeoff. Indeed, the tail rotor tones are very distinct in the spectra of Fig. 16.

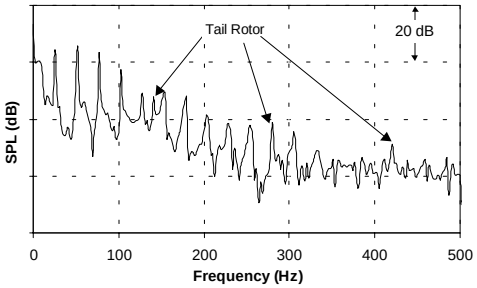

(a) Port Microphone (Retreating Side)

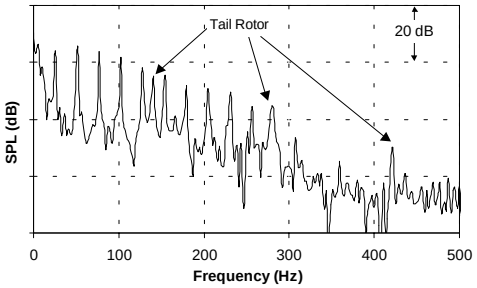

(b) Centerline Microphone

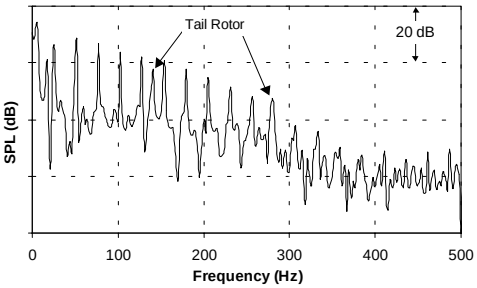

(c) Starboard Microphone (Advancing Side)

Figure 15. Sikorsky S-76 level flight at 136 knots, 492 ft altitude, 3200 ft uprange of mics.

Sikorsky S-76 – Approach

Figure 17 shows the 1-D spectra for the three microphones for a 6-deg, 74 kt approach of the Sikorsky S-76. Helicopter approach noise is typically dominated by blade-vortex interaction noise (BVI) as the main rotor blade tip vortices intersect with the main rotor blades in descent. The three spectra in Fig. 18 indeed show sharp peaks for almost every multiple of the main rotor BPF up to 500 Hz. These peaks rise approximately 10 to 20 dB above the noise floor. The tail rotor BPF can be identified. It can also be observed

that the sound pressure levels are lower for the centerline microphone, especially at the tail rotor frequency.

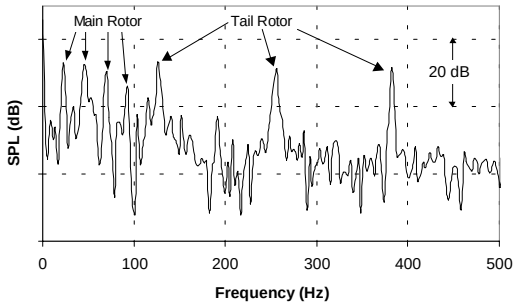

(a) Port Microphone (Retreating Side)

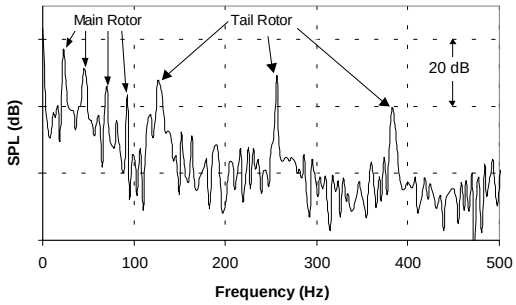

(b) Centerline Microphone

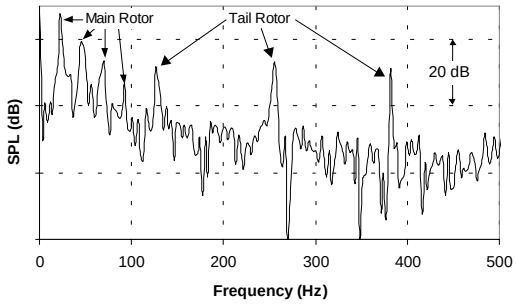

(c) Starboard Microphone (Advancing Side)

Figure 16. Sikorsky S-76 takeoff at 74 knots, 1500 ft uprange of mics.

Two Dimensional Spectra

Boeing MD902 Explorer – Level Flight

Figures 18 (a), (b), and (c) show the 2-D spectra from the Boeing MD 902 level flight data. These spectra exhibit a similar pattern to the simulated signal spectrum in Fig. 6(b), but with less power in the harmonics above the third.

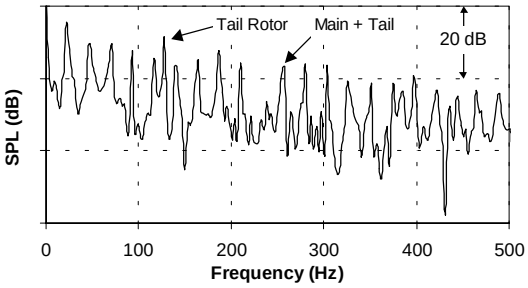

(a) Port microphone (retreating side)

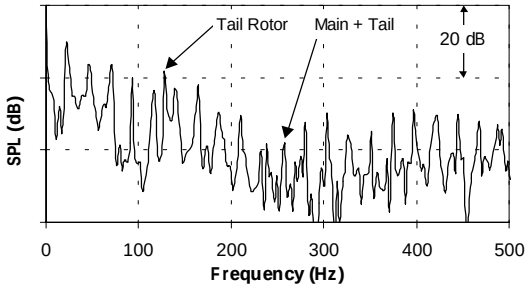

(b) Centerline microphone

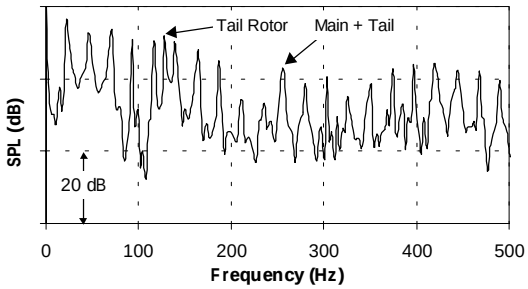

(c) Starboard microphone (advancing side)

Figure 17. Sikorsky S-76 6-deg approach at 74 kts, 3200 ft uprange of mics.

Diagonals are superimposed on the spectra in Figures 18 (a), (b), and (c): one represents the center or main diagonal of the spectrum, and the other cuts through the fundamental BPF of the main rotor. The center diagonals and the fundamental BPF diagonals for the three microphones are plotted in Fig. 19.

The center diagonal of the 2-D spectrum is equivalent to the 1-D Fourier transform of the signal. It contains information from all frequencies present in the signal. The main rotor diagonal, in theory, would give information only from the main rotor BPF and harmonics.

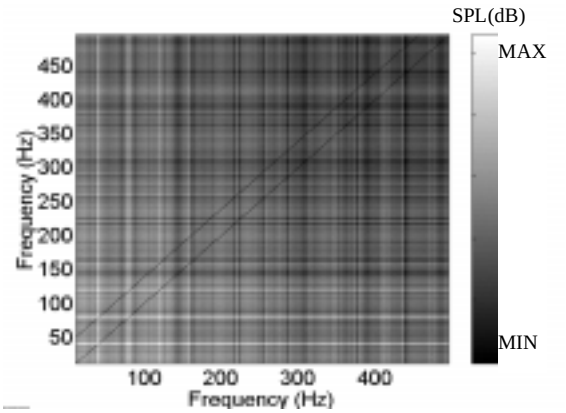

(a) Power Spectrum, Port Mic

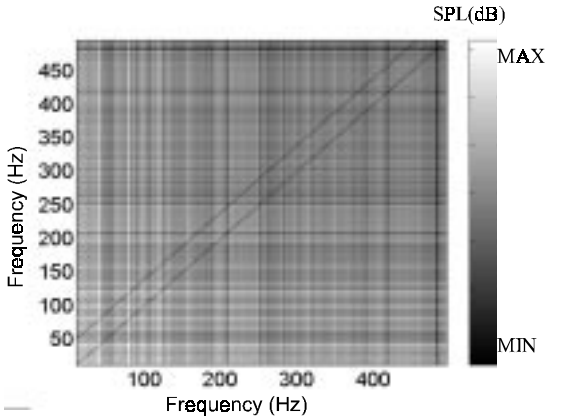

(b) Power Spectrum, Centerline Mic

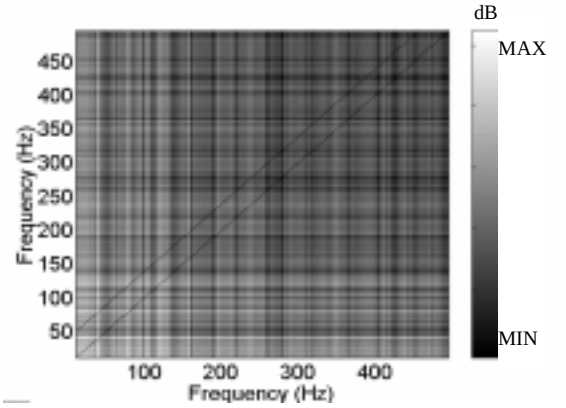

(c) Power Spectrum, Starboard Mic

Figure 18. Boeing MD902 Explorer 2-D spectra for level flight at 115 knots, 500 ft altitude.

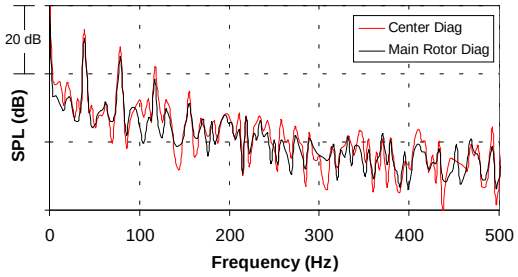

(a) Port Microphone (Retreating Side)

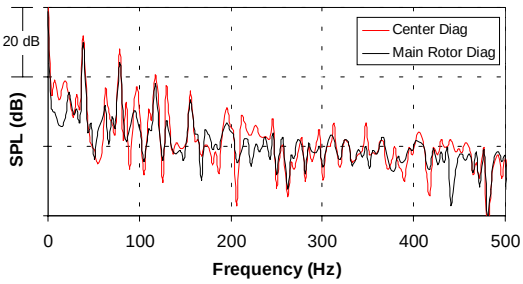

(b) Centerline Microphone

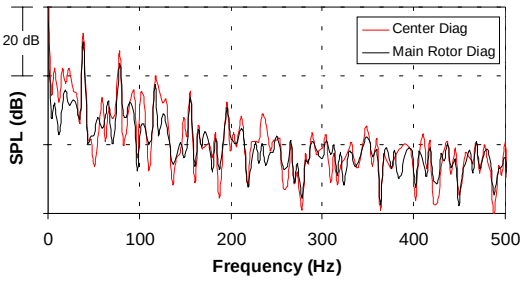

(c) Starboard Microphone (Advancing Side)

Figure 19. Boeing MD 902 level flight, center and main rotor BPF diagonals from 2-D spectra.

The main rotor diagonals (solid lines) in Fig. 19 show a decrease in SPL of up to 14 dB for frequencies not associated with the main rotor BPF. For example, a tone around 130 Hz in Fig. 19(b) is reduced by 10 dB from the center to the main rotor diagonal. The main rotor harmonics up to 4 BPF maintained their SPL within 4 dB from the center diagonal. These observations indicate that the main rotor diagonal indeed contains mostly information associated with the main rotor BPF. This information could be useful in analysis of noise generated by the main rotor as it reduces extraneous noise that is included in the overall spectrum.

Sikorsky S-76 – Level Flight

Figure 20 shows the 2-D autocorrelation and power density spectra for a level flight of the Sikorsky S-76. The autocorrelations and spectra are calculated using a block length containing ten main rotor periods. The spectra of Figs. 20 (a), (b), and (c) show higher SPL on the advancing side of the helicopter rotor.

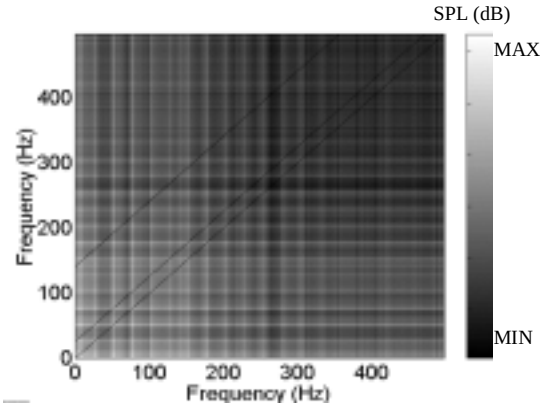

(a) Power Spectrum, Port Mic

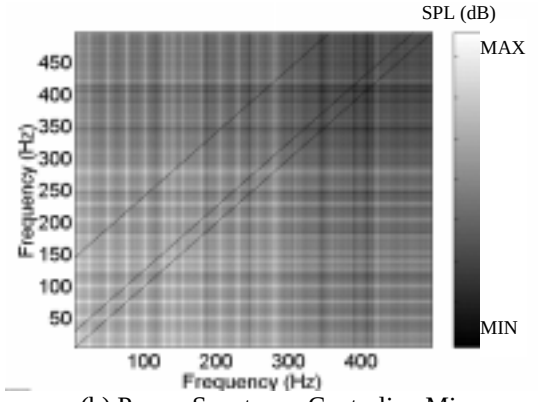

(b) Power Spectrum, Centerline Mic

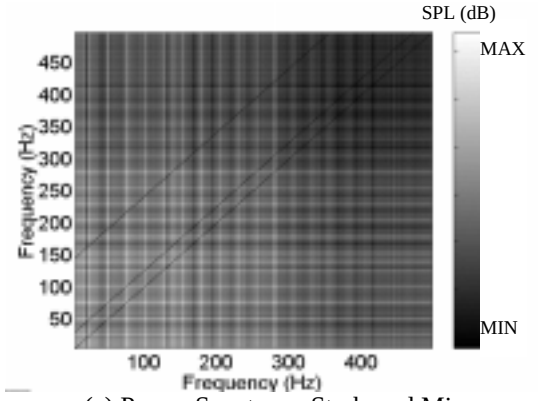

(c) Power Spectrum, Starboard Mic

Figure 20. Sikorsky S-76 level flight at 136 knots, 492 ft altitude.

The center, main rotor BPF and tail rotor BPF diagonals are marked on the spectra of Figs. 20 (a), (b), and (c). The center and main rotor diagonals are plotted together in Fig. 21, and the center and tail rotor diagonals are plotted together in Fig. 22.

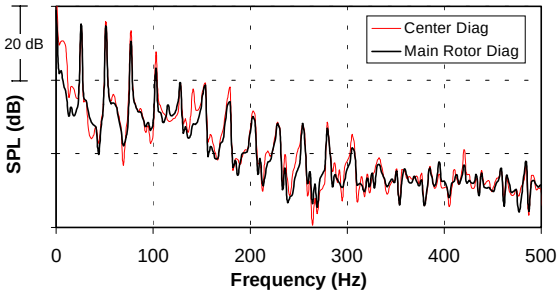

(a) Port Microphone (Retreating side)

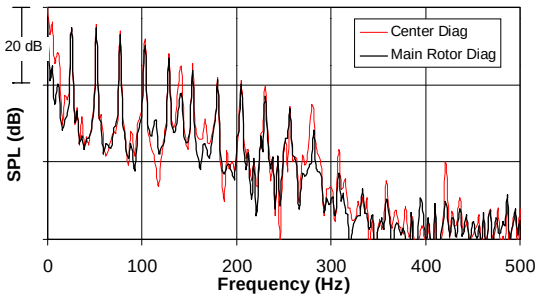

(b) Centerline Microphone

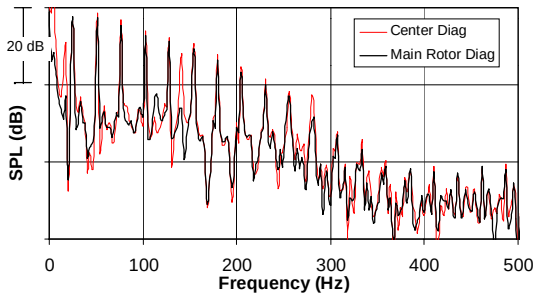

(c) Starboard Microphone (Advancing side)

Figure 21. Center and main rotor diagonals from 2-D spectra, Sikorsky S-76 level flight at 136 kts.

The main rotor diagonals shown in Fig. 21 show a marked decrease in the SPL at the tail rotor frequencies. This decrease is especially notable in Fig. 21(c), the microphone located on the advancing side of the rotor, where the tail rotor BPF around 140 Hz decreases by almost 14 dB. Note that at 2BPF of the tail rotor, the reduction is not as great. This happens to be 11 BPF of

the main rotor, therefore the remaining power should be the contribution of the main rotor at that frequency.

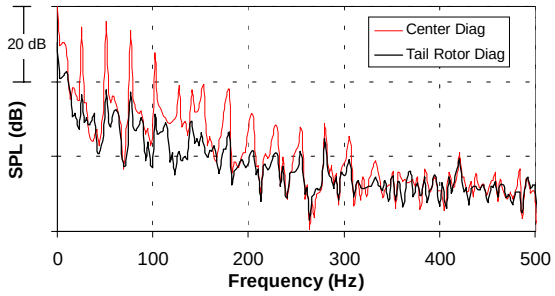

(a) Port microphone (Retreating side)

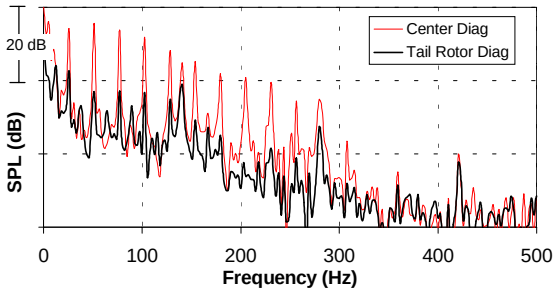

(b) Centerline microphone

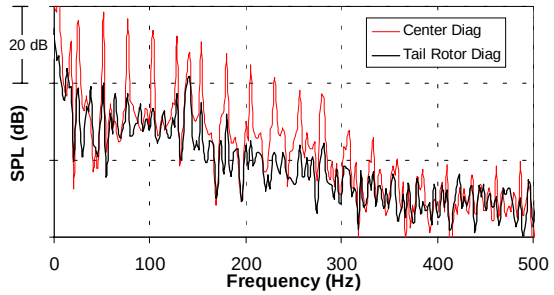

(c) Starboard Microphone (Advancing side)

Figure 22. Center and tail rotor diagonals from 2-D spectra, Sikorsky S-76 level flight, 136 kts.

The diagonals shown in Fig. 22 show a dramatic decrease in SPL of the main rotor tones. The tail rotor diagonals should be representations of the noise contributions of the tail rotor to the overall spectra. The reduction in the tail rotor tones is thought to be related to main rotor-tail rotor interaction.

Sikorsky S-76 – Takeoff

The 2-D power spectra for a Sikorsky S-76 are shown in Fig. 23. These are calculated using one data block, the length of which contains exactly eight periods of the main rotor blade passage. The spectra of Fig. 23 show the dominant tail rotor peaks, as seen in Fig. 16.

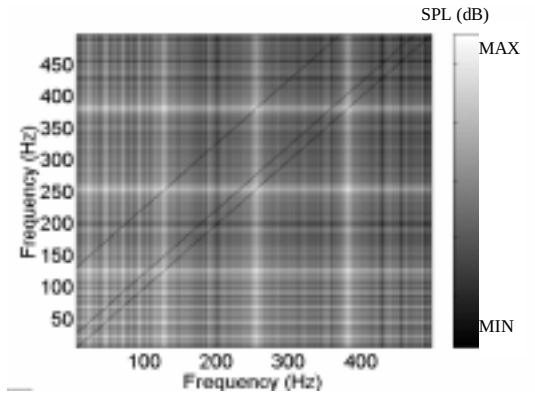

(a) Port Microphone (Retreating Side)

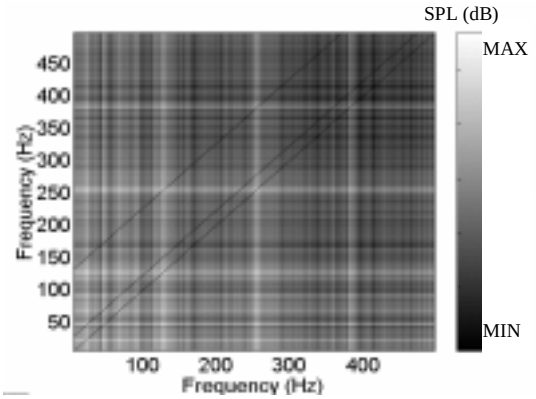

(b) Power Spectrum Centerline Mic

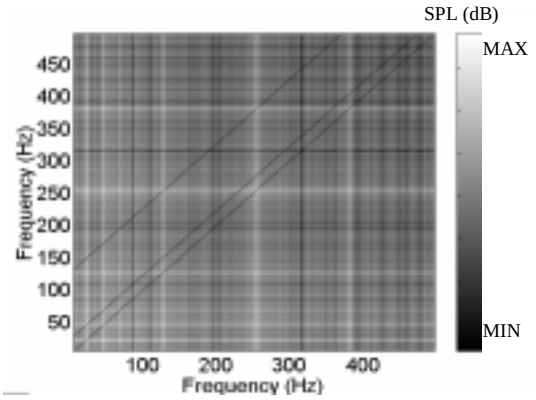

(c) Power Spectrum, Starboard Mic

Figure 23. Sikorsky S-76 takeoff at 74 knots.

Figure 24 shows that the tail rotor tones are greatly reduced, while the main rotor tones are diminished by 0 to 4 dB. This information may be useful in studying main rotor-tail rotor interaction noise, as some tones

appear in the main rotor diagonals of Fig. 24. Specifically, around 230 Hz and 360 Hz, the main rotor diagonal intersects tones whose frequencies are related to both the main and tail rotor.

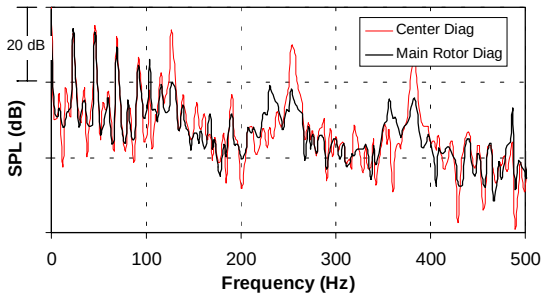

(a) Port Microphone (Retreating side)

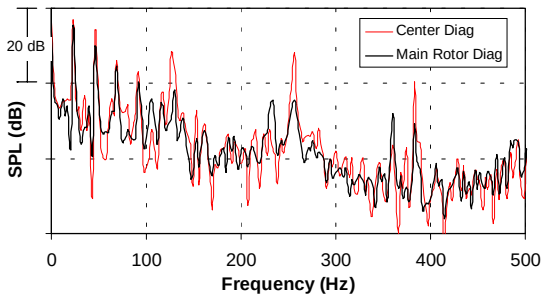

(b) Centerline Microphone

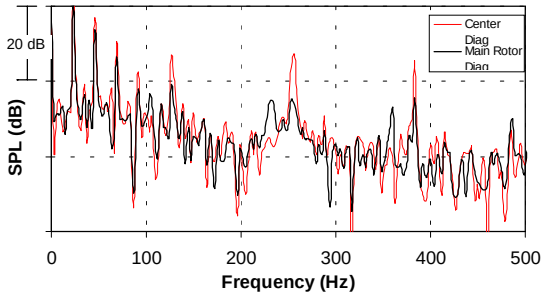

(c) Starboard Microphone (Advancing side)

Figure 24. Center and main rotor diagonals from 2-D spectra, Sikorsky S-76 takeoff at 74 knots.

Diagonals going through the center, main rotor BPF, and tail rotor BPF are marked on the spectra of Fig. 23. The center and main rotor diagonals are shown superimposed in Fig. 24.

The center and tail rotor diagonals for the spectra of Fig. 23 are shown in Fig. 25. Main rotor tones are greatly reduced, while tail rotor tones maintain their amplitude very closely. There are no instances of tone generation such as those seen in Fig. 24 at 230 and 360 Hz in the tail rotor diagonals.

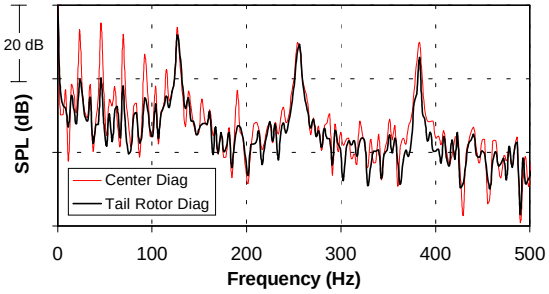

(a) Port Microphone (Retreating side)

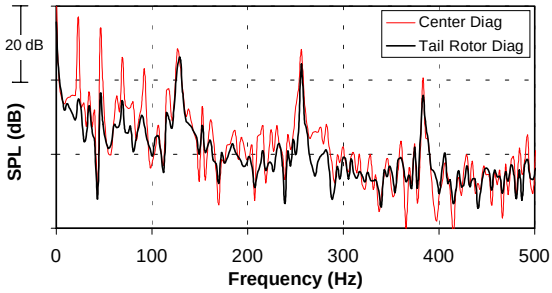

(b) Centerline Microphone

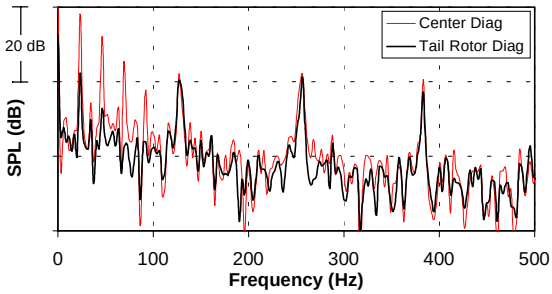

(c) Starboard Microphone (Advancing side)

Figure 25. Center and tail rotor diagonals from 2-D spectra, Sikorsky S-76 takeoff at 74 knots.

Sikorsky S-76 – Approach

The 2-D spectra for the three microphones for a Sikorsky S-76 approach are shown in Fig. 26. The data block length used contains eight periods of the main rotor blade passage. The spectra shown in Figs. 26 (a), (b), and (c) also reflect higher levels on the starboard side.

The superimposed center and main rotor diagonals are shown in Fig. 27. As expected, the main rotor tones are

practically undiminished, while the first and third harmonics of the tail rotor are reduced considerably.

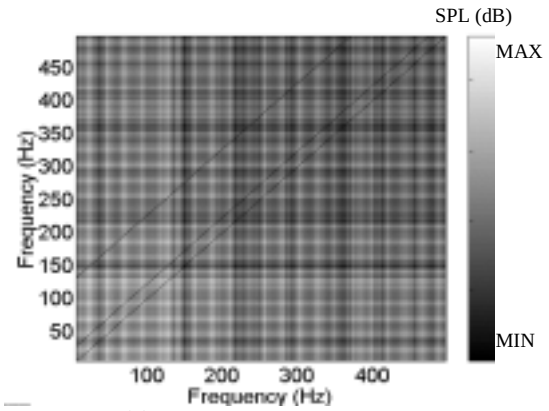

(a) Power Spectrum, Port Mic

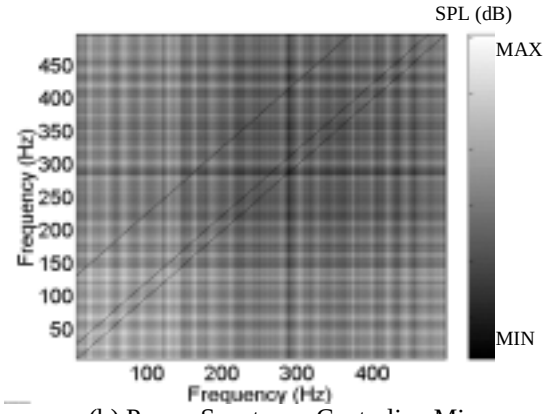

(b) Power Spectrum, Centerline Mic

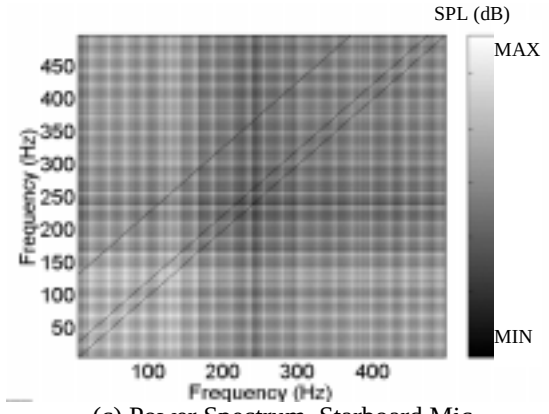

(c) Power Spectrum, Starboard Mic

Figure 26. Sikorsky S-76 6° approach, 74 kts.

Approach noise is generally a main rotor-dominated signature, therefore looking for tail rotor noise during approach may be of interest. The center and tail rotor diagonals for the approach condition are shown in Fig. 28. The main rotor tones are reduced by about 10 dB for the first seven harmonics, while most of the tail rotor tones retain much of their amplitude. However, the centerline microphone shows a tail rotor diagonal with an amplitude approximately 15 dB lower than the main rotor diagonal. Referring to the 1-D spectrum of the centerline microphone in Fig. 17(b), it is obvious that the tail rotor BPF at 130 Hz has a strong presence in the spectrum. Unlike the port and starboard microphones, the 2BPF tail rotor tone is in the noise floor for the centerline microphone. This 2BPF tone is the first tone expected in the tail rotor diagonals of Fig. 27. Therefore, the first expected tone in Fig. 28(b) is in the noise floor.

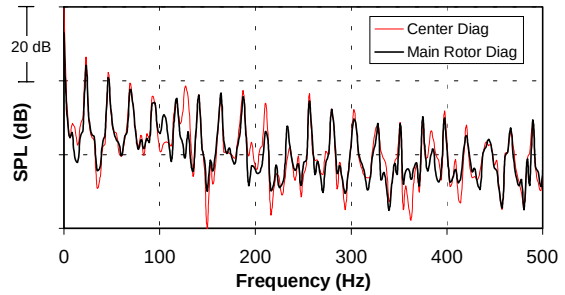

(a) Port Microphone (Retreating side)

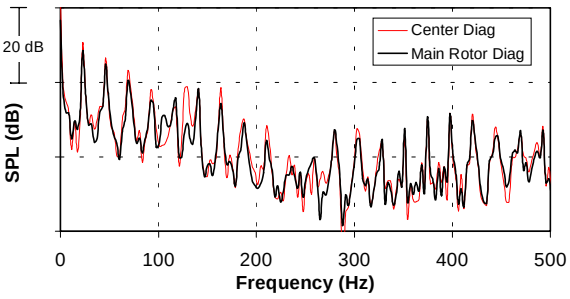

(b) Centerline Microphone

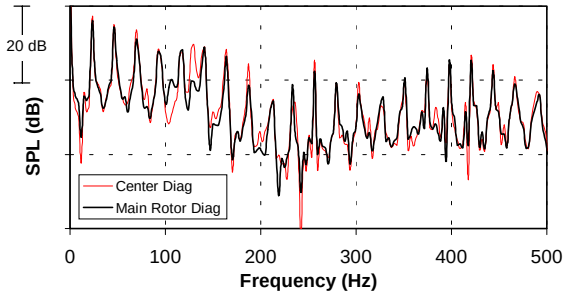

(c) Starboard Microphone (Advancing side)

Figure 27. Center and main rotor diagonals from 2-D spectra, Sikorsky S-76 6° approach, 74 kts.

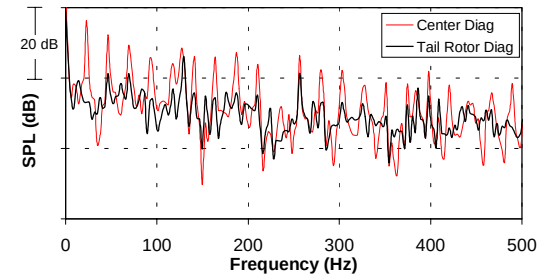

(a) Port Microphone (Retreating side)

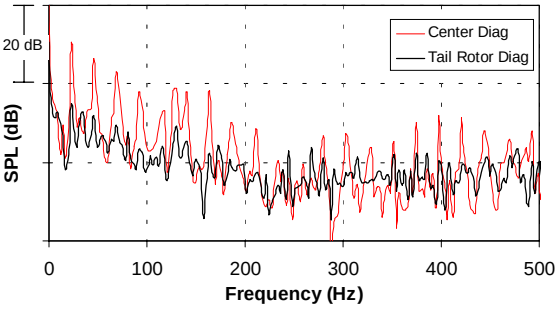

(b) Centerline Microphone

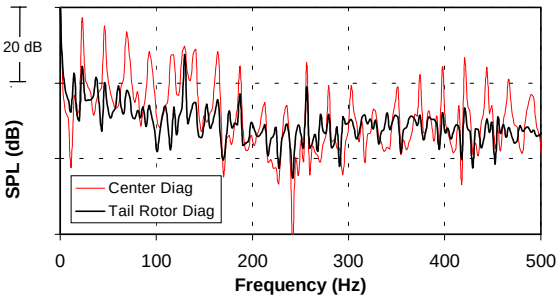

(c) Starboard Microphone (Advancing side)

Figure 28. Center and tail rotor diagonals from 2-D spectra, Sikorsky S-76 6° approach, 74 knots.

VI. CONCLUSIONS

Two-dimensional Fourier analysis of helicopter flyover noise has been found to effectively separate main rotor and tail rotor noise. Since the main rotor and tail rotor frequencies are incommensurate, the resulting signal from a helicopter with a tail rotor is neither periodic nor stationary. A one-dimensional Fourier transform spectrum would not adequately separate these incommensurate frequencies because any data block length chosen would not favor both frequencies.

In this paper, a method has been proposed to separate the main rotor and tail rotor noise spectra. A 2-D correlation function is constructed based on a sample record of the noise in the time domain. The 2-D Fourier transform of the correlation function is then computed. In these 2-D spectra, the main rotor and tail rotor noise spectra are separated from each other on well-defined lines parallel to the center diagonal. This method, based on ideas suggested in ref. [4], can separate more than two frequencies as long as they are relatively prime and incommensurate.

Data from a helicopter flight test has been analyzed using 2-D Fourier analysis. The test aircraft were a Boeing MD902 Explorer (no tail rotor) and a Sikorsky S-76 (4-bladed tail rotor). The results show that the main rotor and tail rotor signals can indeed be separated in the 2-D Fourier transform spectrum. The separation occurs along the diagonals associated with the frequencies of interest. In most cases shown, the main rotor diagonal is a spectrum dominated by main rotor tones, and the tail rotor diagonal is dominated by tail rotor tones.

There is some unexpected reduction in tail rotor tones in some cases, which could be related to main rotor-tail rotor interaction noise. Information for this type of noise, which is a function of both main rotor and tail rotor frequencies, could also be contained in diagonals corresponding to both frequencies. Looking for evidence of main rotor-tail rotor interaction noise in the 2-D spectrum of helicopter noise would be an interesting topic for future work.

This method could have applications besides helicopter noise analysis, for example, system identification, monitoring systems, or prediction validation. By sweeping through all the diagonals in the 2-D spectrum, it may be possible to identify noise sources of interest for system identification. For use in a monitoring system, the diagonal representing the fundamental frequency of a rotating part could be monitored for changes in its periodic motion. To validate noise predictions, one could check for changes in the diagonals of frequencies that are being simulated in the prediction code. Although only the amplitudes of the 2-D spectra are shown in this paper, a study of the phase relationships in the 2-D spectra could also be useful in these applications. In all these examples, 2-D Fourier analysis allows frequencies of interest to be separated from the rest of the signal without filters, while retaining access to the rest of the frequency information.

VII. ACKNOWLEDGEMENTS

Technical tasks described in this document include tasks supported with shared funding by the U.S.

rotorcraft industry and government under the RITA/NASA Cooperative Agreement No. NCCW-0076, Advanced Rotorcraft Technology, Aug. 15, 1995.

The authors would also like to thank Dr. Jay C. Hardin, NASA Langley (ret.), for sharing his ideas on the 2-D Fourier transform analysis.

REFERENCES

1) Santa Maria, Odilyn, "2-D Fourier Analysis of Helicopter Flyover Noise," Masters Thesis, The Pennsylvania State University, December 1998, also NASA TM-1999-209114.

2) Schmitz, F.H., "Rotor Noise," Chapter 2, *Aeroacoustics of Flight Vehicles: Theory and Practice*, Vol. 1, 1991.

3) George, Albert R., and Chou, S.-T., "A Comparative Study of Tail Rotor Noise Mechanisms," American Helicopter Society 41st Annual Forum, Fort Worth, Texas, May 15–17, 1985.

4) Hardin, J.C., and Miamee, A.G., "Correlation Autoregressive Processes with Application to Helicopter Noise," Journal of Sound and Vibration, 142(2), 1990, pp. 191-202.

5) George, Albert R., Chou, S.-T., "A Comparative Study of Tail Rotor Noise Mechanisms," 41st Annual Forum of the American Helicopter Society, Fort Worth, TX, May 15-17, 1985.

6) George, Albert R., Chou, S.-T., "Helicopter Tail Rotor Analyses," NASA Contractor Report, N86-26163, 1986.

7) Shenoy, R.K., Fitzgerald, J.M., Kohlhepp, F., "Aeroacoustic Investigations of Model Tail Rotors in an Anechoic Wind Tunnel," NASA Contractor Report 181809, 1989.

8) Shenoy, Rajarama K., Moffitt, Robert C., Yoerkie, Charles M., Childress, Otis, Jr., "Development and Validation of 'Quiet Tail Rotor Technology," American Helicopter Society International Specialists Meeting on Rotorcraft Acoustics and Fluid Dynamics, Philadelphia, PA, Oct. 15 – 17, 1991.

9) Hardin, Jay C., *Introduction to Time Series Analysis*, NASA Reference Publication 1145, 2nd printing, Nov. 1990.

10) Bendat, Julius S., Piersol, Allan G., Random Data Analysis and Measurement Procedures, 2nd ed., Wiley, 1986.

11) Smith, Gregory L., Miamee, A.G., "A 2-D Power Spectral Study for some Nonstationary Processes," Proceedings of the Second Workshop on Nonstationary Random Processes and their Applications, San Diego, CA, June 11-12m 1995, World Scientific Publishing Co., Pte. Ltd., 1996.

12) Jacobs, Eric W., O'Connell, James M., Conner, David A., Rutledge, Charles K., Wilson, Mark R., Shigemoto, Fred, Chen, Robert T.N., Fleming, Gregory G., "Acoustic Flight Testing of a Boeing MD Explorer and a Sikorsky S-76B Using a Large Area Microphone Array," American Helicopter Society Technical Specialists Meeting for Rotorcraft Acoustics and Aerodynamics, Williamsburg, VA, October 28 – 30, 1997.

13) JanakiRam, Ram D., O'Connell, James M., Frederickson, Daphne E., Conner, David A., Rutledge, Charles K., "Development and Demonstration of Noise Abatement Approach Flight Operations for a Light Twin-Engine Helicopter – MD Explorer," American Helicopter Society Technical Specialists Meeting for Rotorcraft Acoustics and Aerodynamics, Williamsburg, VA, October 28 – 30, 1997.

14) Jacobs, Eric W., Prillwitz, Ronald D., Chen, Robert T.N., Hindson, William S., Santa Maria, Odilyn L., "The Development and Flight Test Demonstration of Noise Abatement Approach Procedures for the Sikorsky S-76," American Helicopter Society Technical Specialists Meeting for Rotorcraft Acoustics and Aerodynamics, Williamsburg, VA, October 28 – 30, 1997.